Macrophage matrix metalloproteinase-12 dampens inflammation and neutrophil influx in arthritis

Journal Article

Author(s):
Bellac, Caroline L.; Dufour, Antoine; Krisinger, Michael J.; Loonchanta, Anantasak; Starr, Amanda E.; auf dem Keller, Ulrich; Lange, Philipp F.; Goebeler, Verena; Kappelhoff, Reinhild; Butler, Georgina S.; Burtnick, Leslie D.; Conway, Edward M.; Roberts, Clive R.; Overall, Christopher M.

Publication date:
2014-10

Permanent link:
https://doi.org/10.3929/ethz-b-000093107

Originally published in:
Cell Reports 9(2), https://doi.org/10.1016/j.celrep.2014.09.006

Article

Cell Reports

Macrophage Matrix Metalloproteinase-12 Dampens Inflammation and Neutrophil Influx in Arthritis

Graphical Abstract

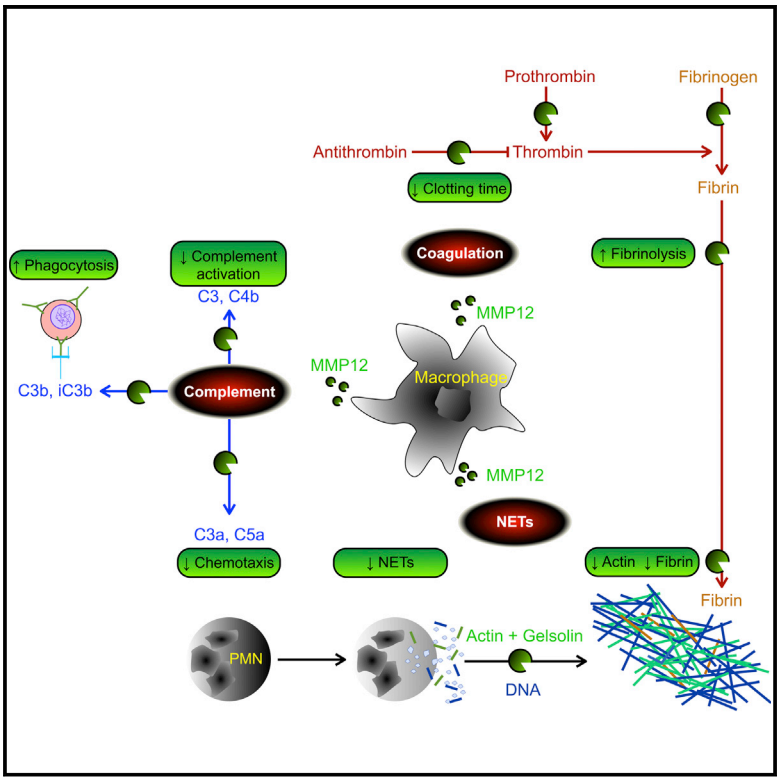

Highlights

Macrophages resolve inflammation via matrix metalloproteinase 12 (MMP12)

MMP12 dampens neutrophil infiltration and clears actin and fibrin from NETs

MMP12 terminates complement activation and increases phagocytosis

By activation of prothrombin in vivo, MMP12 exhibits procoagulant activity

Authors

Caroline L. Bellac, Antoine Dufour, ..., Clive R. Roberts, Christopher M. Overall

Correspondence

chris.overall@ubc.ca

In Brief

Using TAILS proteomics, Bellac et al. now demonstrate that macrophage MMP12 executes multiple protective roles in vivo in inflammation resolution. In arthritis, MMP12 counters neutrophil influx, terminates complement activation, accelerates coagulation, and clears NETs of actin and fibrin to dampen and prepare for the resolution of inflammation.

Bellac et al., 2014, Cell Reports 9, 618–632
October 23, 2014 ©2014 The Authors
http://dx.doi.org/10.1016/j.celrep.2014.09.006

OPEN ACCESS
CellPress

Cell Reports
Article

Macrophage Matrix Metalloproteinase-12 Dampens Inflammation and Neutrophil Influx in Arthritis

Caroline L. Bellac,[1,2] Antoine Dufour,[1,2] Michael J. Krisinger,[1,3] Anantasak Loonchanta,[1,3] Amanda E. Starr,[1,5] Ulrich auf dem Keller,[1,2] Philipp F. Lange,[1,2] Verena Goebeler,[1,2] Reinhild Kappelhoff,[1,2] Georgina S. Butler,[1,2] Leslie D. Burtnick,[1,4] Edward M. Conway,[1,3] Clive R. Roberts,[1,2] and Christopher M. Overall[1,2,5,*]

[1]Centre for Blood Research
[2]Department of Oral Biological and Medical Sciences
[3]Department of Medicine
[4]Department of Chemistry
[5]Department of Biochemistry and Molecular Biology
University of British Columbia, Vancouver, BC V6T 1Z3, Canada
*Correspondence: chris.overall@ubc.ca
http://dx.doi.org/10.1016/j.celrep.2014.09.006

SUMMARY

Resolution of inflammation reduces pathological tissue destruction and restores tissue homeostasis. Here, we used a proteomic protease substrate discovery approach, terminal amine isotopic labeling of substrates (TAILS), to analyze the role of the macrophage-specific matrix metalloproteinase-12 (MMP12) in inflammation. In murine peritonitis, MMP12 inactivates antithrombin and activates prothrombin, prolonging the activated partial thromboplastin time. Furthermore, MMP12 inactivates complement C3 to reduce complement activation and inactivates the chemoattractant anaphylatoxins C3a and C5a, whereas iC3b and C3b opsonin cleavage increases phagocytosis. Loss of these anti-inflammatory activities in collagen-induced arthritis in *Mmp12*$^{-/-}$ mice leads to unresolved synovitis and extensive articular inflammation. Deep articular cartilage loss is associated with massive neutrophil infiltration and abnormal DNA neutrophil extracellular traps (NETs). The NETs are rich in fibrin and extracellular actin, which TAILS identified as MMP12 substrates. Thus, macrophage MMP12 in arthritis has multiple protective roles in countering neutrophil infiltration, clearing NETs, and dampening inflammatory pathways to prepare for the resolution of inflammation.

INTRODUCTION

The inflammatory response to tissue damage involves a fine interplay of different pathways and mediators involving the coagulation cascade, complement system, acute-phase reactants, and innate and adaptive immune cells. This coordinated process ensures that pathogens and damaged tissue are removed and healing commenced to restore tissue homeostasis. Unresolved inflammation contributes to chronic inflammatory diseases, such as rheumatoid arthritis. Macrophages play a dominant role in innate immunity (Galli et al., 2011; Geissmann et al., 2010; Houghton et al., 2009; Marchant et al., 2014). Early in inflammation, resident macrophages recognize foreign or damaged material and secrete proinflammatory mediators that recruit polymorphonuclear neutrophils. Infiltrating neutrophils phagocytize microorganisms and secrete chemokines. Later, cell debris and apoptotic neutrophils are cleared by macrophage phagocytosis. The influx of neutrophils is partially halted through chemokine inactivation by matrix metalloproteinase (MMP) proteolytic processing (Dean et al., 2008) and by phagocytosis-derived signals (Soehnlein and Lindbom, 2010). Apoptotic neutrophils display specific efferocytosis "eat-me" signals, whereas nonspecific opsonization by acute-phase reactants, including complement C3b and iC3b, enhances phagocytic removal of opsonized material and cells. Macrophage protease activity is crucial for phagocytosis and proinflammatory functions, but the in vivo roles of individual macrophage proteases over time in resolving inflammation are unclear.

Whereas MMPs are canonically considered destructive and proinflammatory, beneficial roles for the macrophage-specific matrix metalloproteinase-12 (MMP12) in inflammation and immunity are known: *Mmp12*$^{-/-}$ mice show exacerbated inflammation in lipopolysaccharide-induced lung inflammation (Dean et al., 2008) and increased mortality upon bacterial (Houghton et al., 2009) and viral infections (Marchant et al., 2014). In the absence of MMP12, development of experimental autoimmune encephalomyelitis is accelerated and is associated with cytokine and chemokine dysregulation (Goncalves DaSilva and Yong, 2009). However, MMP12 deficiency reduces neuroinflammation in aged mice by decreasing the recruitment of bone marrow-derived microglia to the brain (Liu et al., 2013). Thus, MMP12 can exhibit both proinflammatory and anti-inflammatory activity in a tissue- or disease context-dependent manner.

Previous studies have focused on the cleavage of extracellular matrix (ECM) substrates by MMP12 (Gronski et al., 1997). However, genetic overexpression introduces a protease at non-physiological levels or in tissues or cells where the protein is not normally found. In contrast, protease knockout tissues

can be directly compared with wild-type tissues expressing physiological or pathological relevant amounts of the protease. Our proteomic technique, terminal amine isotopic labeling of substrates (TAILS) using iTRAQ isotopic labels, enables system-wide analysis of proteolytic events in tissues where all components are present at relevant levels in vivo (auf dem Keller et al., 2013) as well as substrate identification of specific proteases in complex cellular proteomes and secretomes (auf dem Keller et al., 2010; Kleifeld et al., 2010; Prudova et al., 2010). Substrates and their cleavage sites are identified by relative quantification of iTRAQ-labeled N-terminal peptides, including protease-generated neo-N-termini, by comparing protease-expressing to protease-null samples by tandem mass spectrometry (MS/MS).

We report multiple anti-inflammatory roles for MMP12 that are executed through cleavage of substrates that were identified in a proteomic screen using TAILS analysis of secretomes from fibroblasts and TNF-α-treated macrophages incubated with MMP12, and in peritonitis in *Mmp12*$^{+/+}$ versus *Mmp12*$^{-/-}$ mice. Prothrombin was activated by MMP12, and eight complement components were identified as in vivo MMP12 substrates. We show that macrophage MMP12 promotes resolution of inflammation by cleaving C3 to dampen complement activation, MMP12 inactivates C3a and C5a chemoattractants to reduce inflammatory cell infiltration, and together these activities act in concert with iC3b and C3b cleavage, which increases phagocytic clearance of apoptotic cells and foreign material. These anti-inflammatory roles of MMP12 were validated in collagen-induced arthritis; in the absence of MMP12, arthritis was severely debilitating with unresolved inflammation and pronounced infiltration of neutrophils consistent with the loss of MMP12 inactivation of complement. Excessive neutrophil extracellular trap (NET) deposition was found in the joints that contained large amounts of embedded actin and fibrin that are not normally present (Brinkmann et al., 2004). Thus, we show unexpected connections between inflammatory protease pathways in vivo for macrophage MMP12, which include procoagulant and anticoagulant roles, as well as the reduction of complement activation. In addition, MMP12 activity leads to a decrease in neutrophil infiltration at 18 days, as well as the removal of fibrin and actin from NETs in inflamed tissue.

RESULTS

Proteomic Identification of New MMP12 Substrates in Inflammation by TAILS

In comparing wild-type mice with protease-knockout mice, proteins may be cleaved either directly by MMP12 or indirectly by proteases that are regulated by MMP12 in the wild-type mice. This can occur following MMP12 cleavage of regulator proteins (e.g., receptors, inhibitors, and other proteases forming the protease web) (Fortelny et al., 2014). Therefore, to identify new biological roles of macrophage MMP12 in inflammation, we adopted a rigorous and integrated three-system proteomics approach. To be designated as a high-confidence candidate substrate, cleaved proteins must be reproducibly identified by the same neo-N-termini in three separate proteomics analyses in two different in vitro proteomics analyses of MMP12-cleaved secretomes that were also identified in vivo by TAILS analysis of inflammation models in wild-type and MMP12 knockout mice. A total of 24 candidates were then confirmed by biochemical cleavage and cell assays.

TAILS identified the MMP12 proteolytic signature after incubation of murine MMP12 with secretomes of *Mmp12*$^{-/-}$ murine embryonic fibroblasts (MEFs) and murine macrophages (RAW264.7). The *Mmp12*$^{-/-}$ MEFs secrete a MMP12-naive proteome enabling high-confidence proteomic substrate discovery to be performed due to a high signal-to-noise isotopic label ratio. RAW264.7 macrophages were stimulated with tumor necrosis factor alpha (TNF-α) to induce expression of inflammation-relevant secreted and plasma membrane proteins. To confirm biologically relevant substrates of MMP12 in vivo, we winnowed the in vitro MMP12 substrates by comparison with cleaved proteins identified in peritoneal inflammatory exudates in *Mmp12*$^{+/+}$ versus *Mmp12*$^{-/-}$ mice. Only cleavage sites and substrates identified by TAILS in more than one in vitro experiment and also in vivo were defined as MMP12 substrates.

In the two biological replicates of MMP12-digested MEF secretomes, we identified 2,974 and 3,230 unique N-terminal peptides of mature protein N termini and cleaved neo-N-termini of secretome proteins (Figures 1A and S1A; Table S1A; Supplemental Results). TAILS also identified high numbers of N-terminal peptides in duplicates of RAW264.7 cell secretomes treated with MMP12 (4,490 and 3,363 unique N-terminal peptides) (Supplemental Results; Figure 1A; Table S1B). To discriminate MMP12 substrates from background cleavage products in the samples before the assay, we used a statistically determined isotope ratio cutoff (wild-type [WT]/knockout [KO]) $\geq$15 or $\leq$ 0.06 (auf dem Keller et al., 2010) for substrates in the RAW264.7 secretomes and $\geq$7.3 or $\leq$0.13 in the MEF screen (Supplemental Results; Figures 1A and S1A; Table S1C) using the software CLIPPER (auf dem Keller and Overall, 2012). In other words, the cleaved peptides identified by the high iTRAQ ratios means that in the absence of MMP12, the cleavage products were undetectable. High-ratio MMP12-cleaved neo-N-terminal peptides were also identified in biological replicates of RAW264.7 secretomes $\pm$TNF-α stimulation using 4plex-iTRAQ TAILS (Supplemental Results; Figure 1A; Table S1D). Notably, 379 cleavage sites were identical in both the fibroblast and macrophage secretomes cleaved by MMP12 (Figure 1B). Hence, these were the highest-confidence substrates having biological relevance in inflammation (Table 1).

To validate the in vitro findings, we injected 4% thioglycollate into the peritoneal cavity of *Mmp12*$^{-/-}$ (n = 8) and *Mmp12*$^{+/+}$ (n = 8) mice to induce peritonitis on two different background strains (B10.RIII and 129Sv/Ev). Most cleavage sites were identified in both mouse strains (Supplemental Results; Table S1E). Macrophage infiltration was higher in the B10.RIII strain at 96 hr, which was selected for further study in two more replicate sets of mice (Table S1F). We considered further only the unique N-terminal peptides from mature protein N termini and cleaved neo-N termini of 260 proteins that were reproducibly identified in two or more of three sets of B10.RIII mouse pairs (Table S1G). Of the peritonitis proteins, 150 were from major Gene Ontology (GO) categories that were highly relevant to the inflammatory response (e.g. inflammatory mediators, coagulation,

A

Number of unique peptides and proteins identified by TAILS

	Fibroblasts (in vitro)		Macrophages (in vitro)		Peritoneal Lavages (in vivo)	
	Exp 1	Exp 2	Exp 1	Exp 2	Exp 1	Exp 2
Mascot search (peptides)	1,963	2,427	3,321	2,597	720	362
X! Tandem search (peptides)	2,523	2,021	3,191	2,884	596	388
Combined searches (peptides)	2,974	3,230	4,490	3,363	897	494
Unique peptides in both experiments	4,298		6174		1,039	
Identified in 2 biological replicates or by at least 2 spectra (peptides/proteins)	1,515/ 591		1535/ 670		124/ 73 494/ 260	
High confidence substrates (peptides/proteins)	828/370		903/447		79/37	

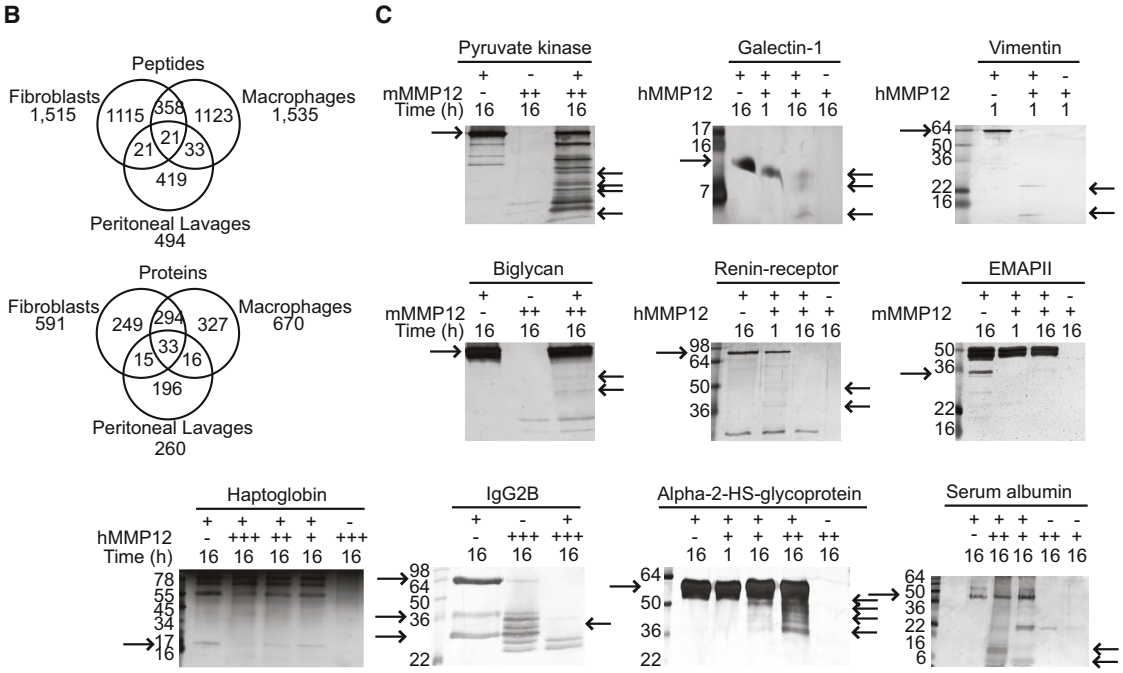

Figure 1. Overview of MMP12 Substrate Discovery by TAILS and Biochemical Confirmation of Substrates

(A) Numbers of unique peptides and proteins identified by TAILS proteomics of MMP12-digested secretomes from *Mmp12*$^{-/-}$ MEFs, macrophages in vitro, and peritoneal lavages of thioglycollate-induced peritonitis in *Mmp12*$^{+/+}$ and *Mmp12*$^{-/-}$ mice in vivo. All experiments were performed as two biological replicates. Only peptides identified more than two times were further considered as candidate substrates and only if they exceeded the statistically determined isotopic ratio cutoffs from MEFs >7.3 or <0.13, macrophages >15 or <0.06, or peritoneal lavages ≥1.2 or ≤0.8 (averaged WT/KO, n = 3).

(B) Venn diagrams of peptide and proteins identified by TAILS.

(C) Biochemical validation of candidate MMP12 substrates. Proteins (left arrow) were incubated with recombinant human (h) or mouse (m) MMP12 at three enzyme/substrate ratios (1:100 [+], 1:10 [++], and 1:5 [+++]); buffer (–), 37°C for 1 hr or 16 hr. Digestion products were separated by 12%–15% SDS-PAGE or 15% Tris-Tricine gels and silver stained. Right arrow, major cleavage products.

complement, phagocytosis, antigen presentation, B and T cell regulation, and ECM remodeling) (Table 1).

In total, 50% (327) of cleaved proteins were common between the fibroblast and macrophage secretomes, but only 64 were identical in peritoneal lavage and cell secretomes, as the majority of the cleaved proteins in the peritoneal lavage were blood plasma derived. Thus, 64 identical substrates with 75 identical cleavage sites were identified by iTRAQ-TAILS both in vitro and in vivo. Thus, the in vivo cleavages most likely directly resulted from MMP12 (Figures 1B and S1B; Tables S1H and S1I). From the isotopic ratios and GO categories, 36 of these were classified as in vivo MMP12 substrates with high relevance in inflammation (24 of which we validated biochemically), including the acute response proteins α1-antitrypsin, α2 macroglobulin, serotransferrin, fibrinogen, albumin, haptoglobin, antithrombin, α2HS-glycoprotein, and eight complement proteins (Tables 2 and S1J).

PICS Analysis of MMP12 Cleavage Sites

To further confirm direct MMP12 cleavage of candidate substrates in vivo, we determined the P6-P6′ cleavage site specificity of MMP12 in vivo and compared this with the optimal cleavage site amino acid preferences determined using proteomic identification of cleavage site specificity (PICS) (Schilling and Overall, 2008). PICS profiles active site amino acid preferences of purified proteases using denatured proteome-derived peptide libraries. We found that for the iTRAQ-labeled neo-N-terminal peptides in vivo having *Mmp12* WT/KO ratios ≥15, the amino acid preferences matched those obtained in vitro by PICS (Figure S1C), supporting the finding that proteins with

Table 1. Gene Ontology of High-Confidence MMP12 Substrates Reproducibly Identified in MMP12-Cleaved Secretomes of Fibroblasts and Macrophages In Vitro and In Vivo from Peritoneal Lavages

GO category	Protein
Stress/ inflammatory mediators	Alpha-1-antitrypsin 1-2
	Alpha-1-antitrypsin 1-4
	Alpha-2-HS-glycoprotein
	Aminoacyl tRNA synthase complex-interacting multifunctional protein 1
	Aminopeptidase B
	Annexin A1
	Apolipoprotein-1
	Beta-2-microglobulin
	Chymotrypsin-like elastase family member 1
	Complement C3
	Coronin-1A
	Extracellular superoxide dismutase [Cu-Zn]
	Fibronectin
	Glucose-6-phosphate 1-dehydrogenase X
	Galectin-1
	Granulins
	Heat shock protein HSP 90-alpha
	Heat shock protein HSP 90-beta
	Hemopexin
	Macrophage migration inhibitory factor
	Mannan-binding lectin serine protease 2
	Mannose-binding protein A
	Peptidyl-prolyl cis-trans isomerase FKBP1A
	Peroxiredoxin-2
	Phospholipase A-2-activating protein
	Serum albumin
	Tyrosine-protein phosphatase non-receptor type 6
Cell migration	Aminoacyl tRNA synthase complex-interacting multifunctional protein 1
	Apolipoprotein-1
	Chloride intracellular channel protein 4
	Coronin-1A
	Destrin
	EMAP-II
	Glutathione peroxidase 1
	Haptoglobin
	Myosin-9
	Septin-2
	Serotransferin
Blood coagulation	Antithrombin-III
	Fermitin family homolog 3
	Fibrinogen alpha polypeptide 2
	Histidine-rich glycoprotein
	Myosin-9
	Pleckstrin
Complement system	Complement C3
	Complement C4
	Complement C5
	Complement factor D
	Complement factor H-related protein
	Complement factor I
	Mannan-binding lectin serine protease 2
	Mannose-binding protein A
Phagocytosis	Alpha-2-HS-glycoprotein
	Calreticulin
	Complement C3
	Coronin-1C
	Mannose-binding protein A
Antigen presentation	Beta-2-microglobulin
	Calreticulin
	Glutathione peroxidase 1
	H-2 class I histocompatibility antigen, L-D alpha chain
	Monocyte differentiation antigen CD14
	Proteasome activator complex subunit 1
	Proteasome subunit beta type-4
T cell regulation	Catenin beta-1
	Coronin-1A
	Heat shock protein HSP 90-alpha
	Myosin-9
	Peptidyl-prolyl cis-trans isomerase FKBP1A
	Peroxiredoxin-2
	Plastin-2
	Purine nucleoside phosphorylase
	Tyrosine-protein phosphatase non-receptor type 6
	1-phosphatidylinositol-4,5-bisphosphate phosphodiesterase gamma-1
	40S ribosomal protein S6
	60S ribosomal protein L22
B cell regulation	B-cell receptor-associated protein 31
	Purine nucleoside phosphorylase
	Tumor protein D52
	Tyrosine-protein phosphatase non-receptor type 6
Immunoglobulin regulation	Fc-binding protein 1
	Gm1418 Anti-VIPase light chain variable region
	Gm1499 Anti-colorectal carcinoma light chain
	Hemopexin
	Ig kappa chain V19-17
	Immunoglobulin kappa-chain
	Tyrosine-protein phosphatase non-receptor type 6
Natural killer cell cytotoxicity	Peroxiredoxin-1
	Tyrosine-protein phosphatase non-receptor type 6
Cell death regulation	Aminoacyl tRNA synthase complex-interacting multifunctional protein
	B-cell receptor-associated protein 31
	Bis(5'-nucleosyl)-tetraphosphatase [asymmetrical]
	Catenin beta-1
	Clusterin
	Elongation factor 1-alpha 2
	Galectin-1
	Glutathione peroxidase 1
	Haptoglobin
	Heat shock 70 kDa protein 1B
	Heterogeneous nuclear ribonucleoprotein U
	Macrophage migration inhibitory factor
	NEDD8-activating enzyme E1 regulatory subunit
	Peroxiredoxin-2
	Programmed cell death 6-interacting protein
	Proteasome activator complex subunit 3
	Protein disulfide-isomerase A3
	Purine nucleoside phosphorylase
	Reticulon-4
	Serine/threonine-protein phosphatase 2A catalytic subunit b isoform
	Serum albumin
	Transitional endoplasmic reticulum ATPase
	Ubiquilin-1
	Ubiquitin-conjugating enzyme E2 Z
	14-3-3 protein eta
	40S ribosomal protein S3a
	40S ribosomal protein S6
Cytoskeleton remodelling	Actin
	Actin-related protein 2/3 complex subunit 1B
	Adenylyl cyclase-associated protein 1
	Alpha-actinin-1
	Alpha-actinin-4
	Coronin-1A
	Destrin
	Drebrin
	F-actin-capping protein subunit alpha-1
	F-actin-capping protein subunit beta
	Fibronectin
	Filamin-A
	Gelsolin
	Glial fibrillary acidic protein
	Macrophage-capping protein
	Myosin-9
	Plastin-2
	Pleckstrin
	Profilin-1
	Radixin
	Ran-specific GTPase-activating protein
	Serotransferrin
	Spectrin beta chain, brain 1
	Vimentin
	14-3-3 protein eta
Extracellular matrix remodelling	Amyloid beta A4 protein
	Biglycan
	Collagen alpha-2(V) chain
	Galectin-3
	Periostin
	Renin-receptor
	Serpin H1
	Transforming growth factor-beta-induced protein ig-h3

All substrates met the following stringent criteria by having isotope ratios of cleaved neo-N-terminal peptides (MMP12/cont) after cleavage of secretomes of MEFs: ratio $\geq$7.3 or $\leq$0.13; macrophages: ratio $\geq$15 or $\leq$0.06; peritoneal lavages: *Mmp12*$^{+/+}$/*Mmp12*$^{-/-}$ ratio $\geq$1.2 or $\leq$0.8; or were biochemically validated as MMP12 substrates.

neo-N-terminal peptide ratios $\geq$15 were direct substrates of MMP12 in vivo. For proteins with lower iTRAQ ratios, differences in the heatmaps crept in, and so these proteins may have been cleaved by other proteases, albeit in a MMP12-dependant manner. To confirm the high ratio substrates, we incubated 24 of these with MMP12 in vitro and found all to be cleaved, confirming our analysis (Figure 1C and later figures).

Acute-Phase and Complement Proteins are MMP12 Substrates

Notable among the in vivo substrates, the acute-phase proteins haptoglobin, α2HS-glycoprotein, immunoglobulin G (IgG) and albumin were biochemically confirmed as new MMP12 substrates (Figure 1C). Many of the substrates identified in vivo showed proteolytic ragging or trimming of the new protein termini by

Table 2. Proteins Identified from N-Terminal Peptides by TAILS in Peritoneal Lavages Collected from *Mmp12*$^{+/+}$ and *Mmp12*$^{-/-}$ Mice

Process	Name	Substrate	IPI	Averaged ratios of neo-N-terminal peptides (*Mmp12* wt/ ko)	Start position of neo N-terminal peptides (P1')	Cleavage site (P1-P1')
Coagulation	Alpha-1-antitrypsin 1-2	*	IPI00129755	1.2	377	P-M
	Alpha-1-antitrypsin 1-3		IPI00123920	1.0, 0.9	36, 50	K-D, G-D
	Alpha-1-antitrypsin 1-4	*	IPI00123924	0.6, 1.1	36, 377	K-D,T-Y
	Inter alpha-trypsin inhibitor	*	IPI00119818	0.8	29	A-E
	Alpha-2-macroglobulin		IPI00624663	0.9, 1.0	706, 708	A-L, A-V
	Antithrombin-III	*	IPI00136642	1.2, 1.6, 2.6	35, 36, 377	G-N, N-P, L-F
	Fibrinogen; alpha	*	IPI00115522	0.7, 0.4, 0.7, 0.8, 1.0	20, 21, 23, 240, 409	T-T, T-D, T-E, K-S, C-S
	Kininogen-1		IPI00114958	0.9	389	R-S
	Pi16 protease inhibitor 16		IPI00113610	1	30	A-L
	Vitamin K-dependent protein C		IPI00113750	1.1	199	R-D
Complement	Complement C3	*	IPI00323624	1.2, 1.2, 0.9	749, 960, 1321	R-S, K-V, R-S
	Complement C4		IPI00131091	1.0	953	R-T
	Complement factor D	*	IPI00116945	1.2, 1.4	26, 212	R-I, S-P
	Complement factor H-related protein	*	IPI00121055	0.8	24	G-E
	Complement factor I		IPI00320675	0.9, 1.0	24, 361	A-S, R-V
	Clusterin	*	IPI00320420	1.2	265	P-A
	Plasma protease C1 inhibitor		IPI00122977	1	471	R-S
	Mannose-binding protein A	*	IPI00131398	0.8	19	S-S
	Fc fragment of IgG binding protein-like	*	IPI00227522	0.7	48	K-C
	Ig kappa chain V19-17	*	IPI00137939	1.2	42	G-D
	Ig kappa chain variable	*	IPI00407273	0.3, 1.7, 1.5	20, 21, 23	A-E, C-D, A-E
	Ig kappa chain V19-14	*	IPI00556799	1.2	57	G-D
	Gm1418 Anti-VIPase light chain variable region	*	IPI00169754	1.2	23	G-E
	Gm1499 Anti-colorectal carcinoma light chain	*	IPI00462809	1.3	23	C-D
	VH coding region	*	IPI00457421	1.3	20	C-E
Acute phase	Alpha-2-HS-glycoprotein	*	IPI00128249	0.7, 0.9, 1.4, 0.9, 0.7, 0.9, 0.7	274, 275, 276, 278, 280, 325, 328	P-A, A-D, D-P, P-A, S-V, G-Q, G-A
	Fetuin-B		IPI00469387	1.0	35	R-S
	Granulins	*	IPI00124640	0.7, 1.2	279, 361	K-E, S-D
	Haptoglobin	*	IPI00409148	1.0, 1.3	103, 323	R-I, C-A
	Hemopexin	*	IPI00128484	0.9. 1.9, 1.2	93, 153, 334	N-P, E-C, N-N
	Histidine-rich glycoprotein	*	IPI00322304	1.5	30	A-L
	Murinoglobulin-1	*	IPI00123223	0.7	727	N-D
	Serotransferrin	*	IPI00139788	0.9, 0.8, 0.9, 2.3	332, 358, 574, 638	R-L, N-S, N-L, F-C
	Serum albumin	*	IPI00131695	0.9, 0.9, 1.0, 3.9, 1.1, 0.8, 0.9, 1.2, 0.9, 1.4, 0.7, 1.4, 1.2, 1.7, 0.9, 0.9, 0.8, 0.9, 1.1, 1.5, 0.9, 1.1, 1.0, 1.2, 0.7, 0.7, 0.6, 0.7, 0.8, 0.9, 1.2, 1.0, 1.6, 1.2, 1.3	27, 82, 86, 87, 89, 106, 107, 108, 148, 149, 155, 160, 201, 208, 224, 267, 269, 271, 272, 273, 343, 414,416, 417, 424, 442, 443, 444, 461, 473, 500, 583, 591, 592, 593	A-H, E-S, N-C, C-D, K-S, R-E, E-N, N-Y, M-C, C-T, N-P, M-G, S-C, D-G, K-C, N-K, E-C, C-H, H-G, D-G, N-Y, K-T, N-C, C-D, G-E, Q-V, V-S, S-T, K-C, C-V, K-C, C-C, T-C, C-F, F-S
	Transthyretin	*	IPI00127560	1.4, 1.2, 0.9	23, 25, 26	P-A, G-A, A-G
	Actin	*	IPI00110850	1.3	356	M-W
	Gelsolin	*	IPI00117167	0.4	408	Y-L
ECM	Epidermal growth factor receptor	*	IPI00121190	2.4	23	G-G
	Extracellular superoxide dismutase [Cu-Zn]	*	IPI00114319	0.8, 0.6, 0.6	20, 21, 23	M-S, S-N, P-G
	Fibroleukin		IPI00310797	0.9	31	E-D
Other	Apolipoprotein A-I	*	IPI00121209	0.7, 1.1, 1.5	32, 184, 201	W-D, R-T, R-L
	Apolipoprotein C-I		IPI00119676	1.0	29	P-D
	Cfhr2 BC026782 protein	*	IPI00462363	0.8	81	C-E
	Cholinesterase	*	IPI00131168	1.3	28	S-H
	Chymotrypsin-like elastase family member 1	*	IPI00171983	1.7	17	S-T
	Maltase-glucoamylase	*	IPI00848693	0.8	58	R-T

Peptide ratios of three different *Mmp12*$^{+/+}$ (WT) and *Mmp12*$^{-/-}$ (KO) pairs are averaged. Start positions of neo-N-terminal peptides are listed by the N-terminal P1′ amino acid and the position within the protein.
Asterisks (*) represent candidate MMP12 substrates that were defined as described in Figure S1B and Tables S1E–S1G.

exopeptidases that wipe evidence of adjacent cleavages. Nonetheless, TAILS identified seven of the canonical serine protease cleavage sites in C3, C4, and factors D and I in the peritoneal inflammatory exudate (Figure 2A) (e.g., C3 was processed at the critical cleavage site ^{748}R↓S^{749} that generates C3a, the anaphylatoxin chemoattractant, and C3b). C3b is the cofactor for the C3 convertase (C3bBb) and C5 convertase (C3bBbC3b), which cleave and activate C3 and C5.

MMP12-dependent cleavage sites in complement were also identified from the neo-N-terminal peptides having high WT/KO ratios in the peritoneal lavages (Figure 2A). Reduced amounts of the factor I-inactivating cleavage of C3b at ^{1320}R↓S^{1321} were found in the wild-type mice, suggesting reduced factor I activity in wild-type mice, but not *Mmp12*$^{-/-}$ mice. Indeed, a cleavage site was found by TAILS in factor I at ^{360}R↓V^{361} in vivo, and in vitro we found MMP12-cleaved factor I (Figure 2B). Biochemical validation of MMP12 cleavage of these complement proteins is shown in Figure 2B. C3a and C5a cleavage was further shown by MALDI-TOF MS (Figure S2A–S2D). Notably, MMP12 cleaved the physiologically important fragments of C3 (C3a, C3b, and iC3b; Figure 2B) at ^{989}Q↓M^{990} as shown by Edman sequencing. Factor D was not cleaved by MMP12 (Figure 2B), providing evidence that MMP12 does not act as a nonspecific protease. In total, MMP12 cleaved eight components of the complement system (Figure 2C).

MMP12 Inactivates C3 and the Opsonin C3b to Reduce Complement Activation

We hypothesized that MMP12 cleavage of C3, C3a, C3b, and iC3b would alter their bioactivity. Human C3-deficient serum is unable to recognize and lyse rabbit erythrocytes, as C3 is required for formation of the C5b-9 membrane attack complex (Figure 2C). C3-deficient serum was reconstituted with intact C3, which led to erythrocyte lysis (Figure 2D). MMP12-cleaved

C3 reduced rabbit erythrocyte lysis >2-fold ($p < 0.01$) (Figure 2D). Hence, MMP12 inactivates C3 to reduce complement activation.

We next assessed the ability of MMP12 to cleave the C3b on cell surfaces. In complement activation, C3 is cleaved to C3b, which covalently binds and opsonizes target cell surfaces. C3b also forms the C3 and C5 convertases (C3bBb and C3bBbC3b) for efficient activation of C3 and C5, respectively, and target-cell lysis. Immobilization of intact C3b on rabbit erythrocytes resulted in ~85% lysis even in highly diluted (0.015 ×) C3-deficient serum (Figure 2E). In contrast, C3b-tagged cells were significantly protected from complement lysis in an MMP12-concentration-dependent manner when later incubated in C3-deficient serum (Figure 2E). Indeed, the inactivation of surface-bound C3b by MMP12 approached the levels of inhibition by the prototypical alternative pathway inhibitors factors H and I (Figure 2E). Thus, MMP12 cleavage of C3 and surface-bound C3b reduces the proinflammatory activation of complement and cell lysis.

Cleavage of C3b and iC3b by MMP12 Increases Phagocytosis

Complement C3b and iC3b are products of C3 that trigger phagocytosis by binding to complement receptors, mainly CR1 for C3b and CR3/4 for iC3b on macrophages. Addition of C3b to stimulated THP1 monocytes significantly increased phagocytosis of microparticles (Figure 2F). Unexpectedly, MMP12-cleaved forms of C3b and iC3b were both significantly stronger mediators of phagocytosis than their intact counterparts (phagocytosis index 1.8 versus 1.3 for C3b; 1.4 versus 1.1 for iC3b; $p < 0.001$). Edman sequencing revealed that the major MMP12 cleavage site in vitro was identical in C3b and iC3b at position ^{989}Q↓M^{990}. Thus, macrophage MMP12 promotes phagocytosis of opsonized cells by generating more potent phagocytosis enhancers from C3b and iC3b and thereby is predicted to promote resolution.

MMP12 Cleavage of C3a Abolishes THP1 Receptor Binding and Calcium Mobilization

The other C3 cleavage product, C3a anaphylatoxin, increases vascular permeability and is a potent stimulator of leukocyte chemotaxis upon binding to the G protein-coupled C3a receptor on a variety of cells, including most leukocytes. THP1 monocytes challenged with C3a had a higher intracellular calcium flux than cells challenged with the monocyte chemokine CCL7 (Figure 2G). Notably, MMP12 potently reduced C3a receptor stimulation as evidenced by a 3-fold reduction in calcium flux (Figure 2G). Edman sequencing and MALDI-TOF MS showed that hMMP12 removed the C-terminal eight amino acids from hC3a at ^{740}R↓A^{741} (Figures S2A and S2B) and also removed the five C-terminal amino acids from hC5a (Figures S2C and S2D) at ^{746}D↓M^{747}, which also decreased calcium mobilization (Figure S3E), but to a lesser extent than for cleaved C3a. Thus, macrophage MMP12 inactivates the neutrophil and macrophage chemotactic C3a and C5a anaphylatoxins and is predicted to be anti-inflammatory by reducing neutrophil and then macrophage infiltration in vivo.

MMP12 Decreases Neutrophil Recruitment in Arthritis In Vivo

We assessed the predicted MMP12 termination of proinflammatory complement activation and associated neutrophil and macrophage infiltration in vivo in a second model of inflammatory disease. *Mmp12*$^{-/-}$ mice (129Sv/Ev background) were backcrossed onto the collagen-induced arthritis-susceptible strain B10.RIII. Collagen-induced arthritis involves autoimmunity to type II collagen with synovial hyperplasia, neutrophil and macrophage infiltration, and cartilage degradation resulting in joint dysfunction. Normal hind ankle joints in wild-type ($n = 15$) and *Mmp12*$^{-/-}$ ($n = 14$) mice at day 0 showed no differences in paw edema or histological changes as quantified by a four-point grading scheme (0–4) (data not shown). All mice developed clinical and histological features of arthritis after collagen injection. However, the knockouts exhibited highly significant and dramatically worse disease and showed significantly increased hind ankle widths due to edema versus wild-type animals from day 9 to day 18, when the difference peaked (1.0 mm versus 0.5 mm, $p < 0.05$) (Figure 3A). Wild-type mice had a histological inflammation score of 1.5 on day 18 ($n = 4$), whereas knockout animals showed a uniformly maximum inflammation score of 4 ($n = 4$) (Figure 3B). This was clearly evident in the histological sections comparing the wild-type (Figures 3C, 3D, and S3) and knockout mice (Figures 3E–3H, S4, and S5). Thus, the loss of macrophage-specific MMP12 worsened disease.

Histological analysis showed that inflammation in the joints of *Mmp12*$^{-/-}$ mice at day 18 was associated with extensive tissue destruction and the tissue architecture was severely disrupted. Subchondral bone loss was only evident in the knockouts and was often associated with groups of fibroblastic cells in the extensive inflammatory pannus (Figures 3E, 3G, S4, and S5). Toluidine blue O staining revealed extensive loss of glycosaminoglycan from the joint surfaces, with loss of metachromatic staining to ~30% of the cartilage depth (Figures 3F, 3H, S4D, S4G, and S5), which was not evident in wild-types (Figures 3D, S3, and S5). Notably, cartilage degradation was adjacent the profound neutrophilic joint effusions in the *Mmp12*$^{-/-}$ mice (Figures 3E, 3G, S4A–S4F, and S5).

Strikingly and consistent with our in vivo proteomics analyses showing inactivation by MMP12 of the chemoattractants C3a and C5a in vivo and in vitro, neutrophilic inflammation was virtually absent in the wild-type mice, unlike the knockout mice (Figures 3K, S4, and S5). Indeed, wild-type mice had very few infiltrating cells at all except for one animal, and here the inflammation was dominated by macrophages rather than neutrophils (proportion of stained cells in synovial fields: macrophages, 23% [WT] versus 7% [KO]; neutrophils, 14% [WT] versus 91% [KO]) (Figures 3K and S7). Consistent with the marked neutrophilia in the joints of the knockout mice were large intra-articular accumulations of NETs containing prominent neutrophils that were not observed in the wild-types (Figures 3, 4, S3, and S5), as presented later.

MMP12 Lyses Fibrin Clots In Vitro and In Vivo

Extracellular fibrin, the terminal product of the coagulation system, accumulated prominently in inflamed joints of *Mmp12*$^{-/-}$ mice compared to wild-types (Figures 3I and 3J). MMP12

A Cleavage sites within components of the murine complement system identified by TAILS

Protein	Sequence	IPI	Cleavage sites (P1') identified by TAILS
Complement C3	23-1663	IPI00323624	479, 749, 752, 753, 919, 960, 968, 969, 984, 991,1321
C3a	672-748	IPI00323624	749
C3b	749-1663	IPI00323624	752, 753, 919, 960, 968, 969, 984, 991,1321
iC3b	955-1303	IPI00323624	960, 968, 969, 984, 991
Complement C4b	754-1443	IPI00131091	678, 754, 953, 1448
Complement factor D	26-259	IPI00116945	26, 212
Complement factor H	19-343	IPI00121050	24
Complement factor I	19-603	IPI00320675	24, 361

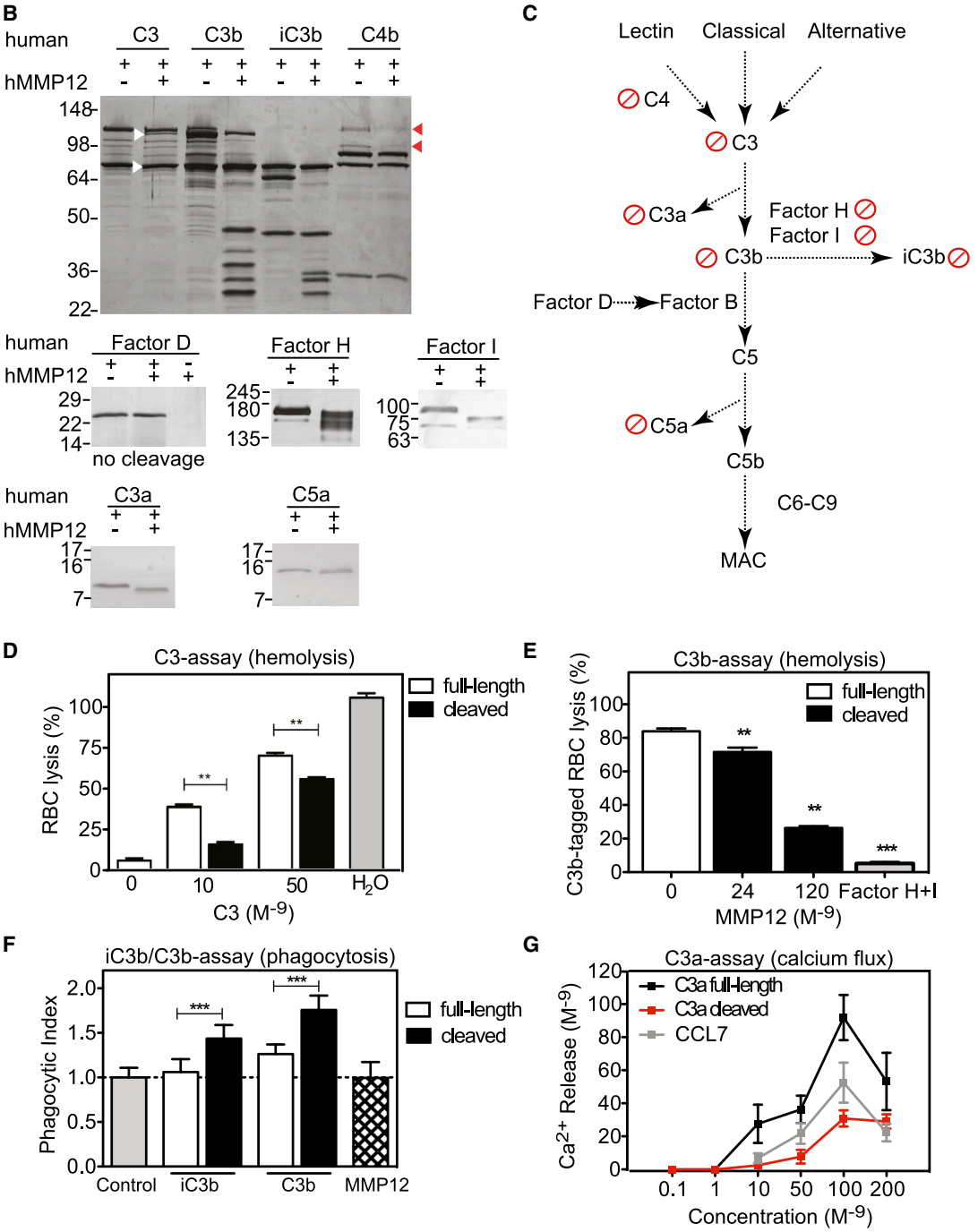

(legend on next page)

cleaves fibrinogen (Hiller et al., 2000). Therefore, we investigated the ability of MMP12 to degrade fibrin. MMP12 lysed fibrin clots in vitro, significantly reducing the clot absorption at 405 nm (A_{405}) to 14% by 2 hr. Marimastat, an MMP inhibitor drug, prevented fibrinolysis ($p < 0.01$) (Figure S6A).

THP1 monocytic cells that were induced to differentiate to M0 macrophages with phorbol 12-myristate 13-acetate (PMA) (at which point they release MMP12) dissolved fibrin clots by 33% at 2 hr and 50% at 4 hr (Figure S6B). The specific MMP12 inhibitor RXP 470.1 prevented all THP1-induced fibrinolysis at 2 hr ($p < 0.01$) and significantly reduced fibrinolysis at 4 hr ($p < 0.01$), revealing the relative importance of MMP12 over other MMPs in the fibrinolytic repertoire of monocytes in vitro and of neutrophils in vivo.

Primary peritoneal macrophages from *Mmp12*$^{-/-}$ mice were also significantly less effective ($p < 0.01$) than those from wild-type mice in fibrin clot lysis in vitro (Figure 3L). As discussed later, MMP12 also cleaved fibrinogen, delaying clotting and hence reducing fibrin generation (Figure S6C). Hence, in the absence of macrophage MMP12 in vivo, fibrin significantly accumulates in NETs and in the intra-articular space in collagen-induced arthritis, revealing the key role of the macrophage and MMP12 in clearing fibrin from inflammatory sites in vivo.

MMP12 Cleaves Actin and Gelsolin, Preventing Extracellular Actin Polymerization in NETs

We identified multiple MMP12 cleavage sites within actin and gelsolin by quantitative proteomic comparison of wild-type versus MMP12-knockout peritonitis samples using TAILS (Figure 4A; Table 2). MMP12 cleaved these substrates in in vitro digests, confirming the in vivo data (Figures 4B and 4C). Extracellular actin filaments are severed and scavenged by the highly abundant plasma gelsolin. Gelsolin consists of six homologous domains (G1–G6) (Figure 4D), each having different functions in regard to calcium and actin binding and in regulating the assembly of actin filaments. Four major MMP12 cleavage products of gelsolin were identified in vitro (Figure 4C), and Edman sequencing revealed that cleavage occurred between the G2 and G3 domains at positions 182 and 282, producing two fragments consisting of the G1 domain plus the linker and the G2 plus G3 domains (Figure 4D).

To assess the functional consequences of gelsolin cleavage, we performed actin polymerization assays. Intact gelsolin nucleates the polymerization of G-actin, resulting in actin-filament growth that was quantified by an increase in light scatter (blue plot in Figure 4E). MMP12 abolished the G-actin nucleation activity of gelsolin, preventing actin polymerization (red plot in Figure 4E). Marimastat reversed the block (Figure S7A). Intact gelsolin also severs filamentous actin, causing actin depolymerization that was quantified by a sharp drop in light scatter upon addition of gelsolin (Figure 4F) and that was also prevented by marimastat (Figure S7B). Notably, MMP12-cleaved gelsolin retained actin-severing activity, although it was reduced. Models of actin polymerization and severing by gelsolin and the effect of MMP12 cleavage are shown in Figures S7C–S7F.

The importance of MMP12 in clearing extracellular actin in the collagen-induced arthritis model was shown in the *Mmp12*$^{-/-}$ mice, where hematoxylin and eosin (H&E) staining showed large clot-like accumulations of extracellular actin that were not present in the wild-type mice (Figures 4G–4I). In addition to staining the actin cytoskeleton of intact cells, Alexa 488-phalloidin prominently stained extracellular actin in these clots in *Mmp12*$^{-/-}$ mice (Figures 4J and 4K). The large deposits of filamentous actin were also associated with DNA in NETs as shown by Hoechst 33358 staining (Figures 4J and 4K). Other components of the NETs included fibrin, especially in the knockout mice (Figures 3I and 3J). The predominance of neutrophils in the NETs suggests that the DNA and actin were from lysed apoptotic neutrophils. Actin in NETs is most unusual: Brinkmann et al. (2004) specifically pointed out that NETs are free of actin. Thus, MMP12 removes filamentous actin from NETs and extracellular deposits in vivo by coordinated actions involving direct cleavage as well as prevention of actin polymerization by cleaving gelsolin while preserving its actin-severing abilities.

MMP12 Cleaves Multiple Components of the Coagulation System

TAILS analysis of peritoneal exudates identified fibrinogen and antithrombin cleavage products (Figure 5A) in the wild-type, but not knockout, mice. Murine MMP12 cleavage of murine

Figure 2. MMP12 Reduces Complement Activation and Increases Phagocytosis

(A) In vivo cleavage sites within complement proteins identified by TAILS analysis of peritonitis lavage in wild-type versus knockouts. Known complement serine-protease cleavage sites are in red.

(B) Biochemical confirmation of human C3, C3a, C3b, iC3b, C4b, and C5a and factors H and I as human MMP12 substrates. C3 cleavage fragments shown by white arrows. Loss of intact C4b is shown by red arrows. Proteins were incubated with MMP12 at 37°C for 16 hr and analyzed on 12% SDS-PAGE or 15% Tris-Tricine gels and silver stained. Factor D was not cleaved by MMP12.

(C) Complement activation occurs by three pathways (classical, lectin, and alternative,) with all three converging with the generation of C3 convertase. This cleaves C3 into C3a and C3b and promotes further cleavage of C5 and the formation of the membrane attack complex (MAC) leading to target-cell lysis. Complement proteins marked with a red slash circle were biochemically validated as MMP12 substrates.

(D) MMP12 reduces complement activation by C3. C3 was incubated ±MMP12, and the digests were assessed for lytic activity against rabbit red blood cells (RBCs) incubated in C3-deficient human serum. Percent RBC lysis is expressed relative to 100% lysis in H_2O. **$p < 0.01$, Mann-Whitney t test.

(E) MMP12 cleavage of C3b bound to the RBC membrane inhibits the alternative pathway. C3b-tagged RBCs were incubated with MMP12 or the inhibitory factors H and I. C3-deficient serum was then added and lysis measured: **$p \leq 0.01$, ***$p \leq 0.001$, Mann-Whitney t test.

(F) MMP12 cleavage of C3b and iC3b increases phagocytosis. PMA-stimulated THP1 cells were incubated with serum-coated fluorescent 2 μm microparticles with full-length or MMP12-cleaved C3b or iC3b and phagocytic uptake of the beads analyzed by fluorescence-activated cell sorting. Cleaved C3b and iC3b were more potent mediators of phagocytosis. ***$p < 0.001$, Mann-Whitney t test.

(G) MMP12 cleavage of C3a reduces C3a receptor activation. C3a triggers dose-dependent intracellular calcium mobilization that exceeded the response by CCL7 and that was lost by MMP12 cleavage. *$p < 0.05$, Mann-Whitney t test.

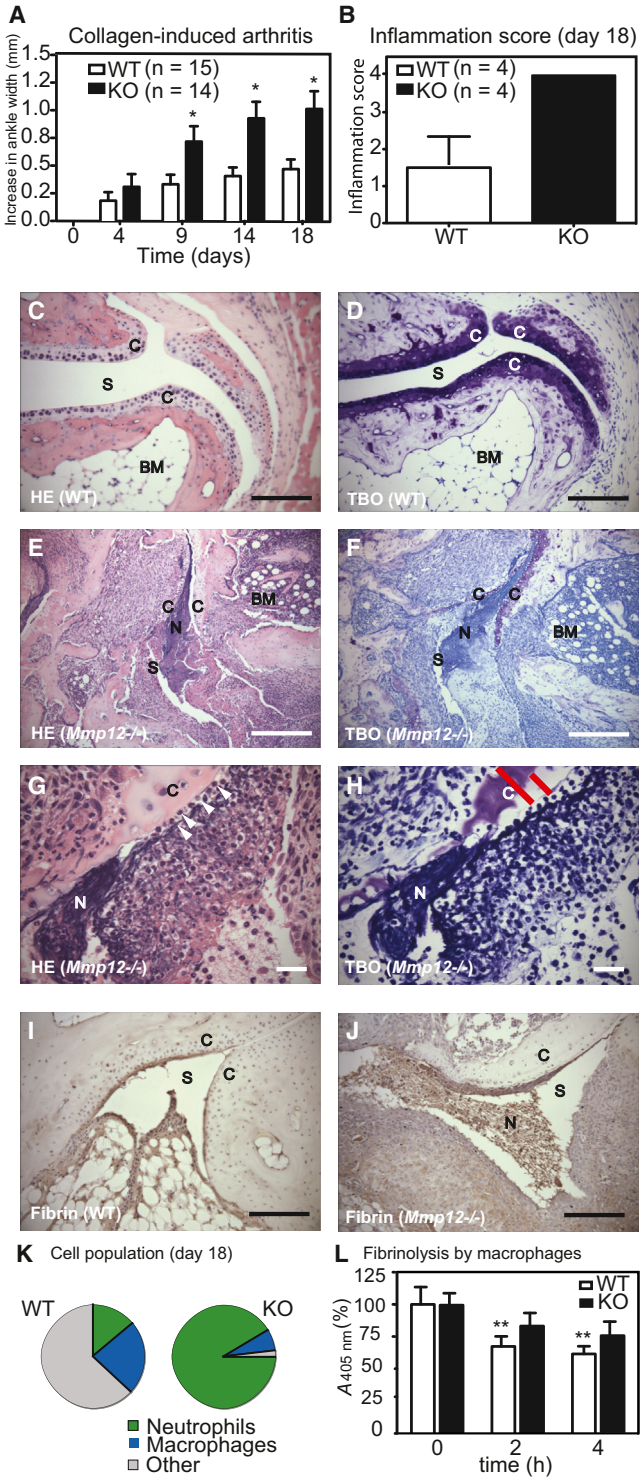

Figure 3. MMP12 Is Protective in Collagen-Induced Arthritis

(A) *Mmp12*$^{-/-}$ mice developed more severe hind ankle swelling than wild-type controls. Increase in ankle width in wild-type (WT) and knockout (KO) mice after onset (day 0 = 21 days after immunization with bovine type II collagen). Values are mean ± SEM. *$p < 0.05$, Mann-Whitney t test.

(B) Scoring of inflammatory infiltration in hind ankle joints at day 18 demonstrated a maximal score of synovial inflammation in all knockout mice.

(C and D) Histological analysis of hind ankle joints at day 18 in wild-type mice with collagen-induced arthritis. Only mild synovial inflammatory cell infiltration was seen using hematoxylin and eosin (HE) staining (C) and with no cartilage damage shown by Toluidine blue O (TBO) staining for proteoglycan (D). C, cartilage; S, synovial space; BM, bone marrow. High-resolution click to zoom imaging.

(E and F) *Mmp12*$^{-/-}$ mice with collagen-induced arthritis at day 18 showed massive inflammatory infiltration (E), including invasion of the joint and marrow spaces, neutrophil NETs (N), and marked loss of joint architecture and proteoglycan content (F).

(G and H) Neutrophil NETs and neutrophil-rich synovial inflammation were frequently seen close to the cartilage (G, white arrows) that was associated with loss of cartilage proteoglycan in *Mmp12*$^{-/-}$ mice (H). Red bars in (H) show depth of intact and proteoglycan-depleted cartilage.

(I and J) Immunostaining for fibrin in wild-type (I) and *Mmp12*$^{-/-}$ (J) ankle joint synovial spaces showed fibrin along the synovial lining in WT mice. In knockout mice, fibrin was in neutrophil-rich effusions and NETs (N) within the joint space.

(K) Inflammatory cell population differences in ankle joints of wild-type and knockouts. Neutrophil numbers are strongly elevated in synovial inflammation in *Mmp12*$^{-/-}$ mice: 91% neutrophils and 7% macrophages versus wild-types having 14% neutrophils and 23% macrophages.

(L) MMP12 mediates fibrinolysis. Incubation of fibrin clots with peritoneal macrophages resulted in clot lysis as shown by the decrease in A_{405} nm (A_{405} = 100% at 0 hr). *Mmp12*$^{-/-}$ macrophages were significantly less efficient in fibrinolysis than wild-types **$p < 0.01$, Mann-Whitney t test.

(C)–(F), (I), and (J), original magnification ×200; scale bar, 100 μm. (G) and (H), original magnification ×630; scale bar, 30 μm.

fibrinogen was confirmed by in vitro digestion of human fibrinogen with human MMP12 (Figure 5B), which reduced clot formation in vitro (Figure S6C).

Thrombin is the key executor in the coagulation cascade, cleaving fibrinogen to fibrin (Figure 5C). Inhibitors such as antithrombin tightly control thrombin activity. In the peritoneal lavages, TAILS identified antithrombin neo-N-terminal peptides with isotopic ratios showing cleavage by MMP12 in vivo (Table 2). Edman sequencing of the major fragment generated by MMP12 cleavage of bovine antithrombin in vitro at ^{376}L↓F^{377} (Figure 5B) confirmed the murine in vivo TAILS data (this cleavage site is conserved in murine, human, and bovine antithrombin). Whereas thrombin preincubated with intact antithrombin showed no activity against a specific chromogenic thrombin substrate, MMP12-cleaved antithrombin lost its ability to inhibit thrombin (Figure 5D). Thus, MMP12 cleaves and inactivates antithrombin by removing the more C-terminal reactive loop center at R^{426} and S^{427}.

As well as promoting thrombin activity by inactivating antithrombin, MMP12 removed the propeptide of prothrombin by precise cleavage at ^{43}R↓A^{44} to generate thrombin, which was active (Figure 5E). Incubation of MMP12 with thrombin showed no further cleavage or degradation (Figure 5B). MMP12 was not as efficient an activator of prothrombin as factor Xa, but nonetheless, MMP12 is an inflammatory activator of prothrombin. The activated partial thromboplastin time is a performance indicator for measuring the efficacy of both the intrinsic and the common coagulation pathways (Figure 5B). We found the activated partial thromboplastin time was significantly prolonged in plasma of *Mmp12*$^{-/-}$ mice (n = 4) compared to *Mmp12*$^{+/+}$ mice (n = 4) (t = 37 s versus 29 s, $p < 0.05$) (Figure 5F), uncovering a procoagulation role for MMP12 in vivo.

DISCUSSION

We identified important regulatory roles for MMP12 and hence macrophages in inflammation. We did so using a comprehensive proteomic strategy to identify new MMP12 substrates in inflammation-relevant secretomes from TNF-α-stimulated or unstimulated macrophages, *Mmp12*$^{-/-}$ MEFs, and in vivo peritonitis samples. Notably, applying multiplex iTRAQ-TAILS to in vivo samples enabled us to globally examine proteolytic events and MMP12-dependent cleavages in vivo, where all of the proteins and their binding partners are present at relevant concentrations. Proteases rarely act in isolation (Fortelny et al., 2014). We report regulatory roles for MMP12 in some of the major proteolytic networks operative in inflammation. Through highly reproducible identification of specific substrate cleavage sites that were found both in vitro and in vivo, we revealed that MMP12 dampens several proinflammatory pathways that facilitate resolution. By targeting multiple substrates from each of the complement and coagulation cascades, we found uncharacterized and unexpected roles for MMP12 in these processes. The complement cascade leads to potent proinflammatory actions in early inflammation, but negative control of the cascade is poorly understood. MMP12 cleaved and inactivated eight complement components in peritonitis. By inactivating C3 and the potent leukocyte chemoattractants C3a and C5a, MMP12 reduced complement activation and disabled the main complement chemoattractant signals for recruiting leukocytes. C3 accounts for tissue damage in arthritis (Wang et al., 2011). Consistent with this, the most striking result of MMP12 deficiency was found in collagen-induced arthritis, where dramatically exaggerated inflammatory responses in vivo were characterized by massive numbers of infiltrating neutrophils and gross destruction of the cartilage and endochondral bone despite the absence of MMP12, a protease traditionally attributed to ECM degradation in inflammation.

Coagulation was enhanced by activation of prothrombin by MMP12 and through cleavage and inactivation of antithrombin; clotting times were significantly prolonged in *Mmp12*$^{-/-}$ plasma compared with normal *Mmp12*$^{+/+}$ plasma. Until this report the only enzyme known to cleave prothrombin to generate thrombin aside from factor Xa is the lectin-pathway activator, MASP2 (Gulla et al., 2010). The inactivation of antithrombin was yet another example of the metalloserpin switch that releases the brake on serine protease cascades as found in vivo for MMP2 in complement activation (auf dem Keller et al., 2013) and for MMP8 in controlling neutrophil chemotaxis by CXCL5 and interleukin-8 activation (Fortelny et al., 2014). Rather than cleavage in the reactive center loop, antithrombin is cleaved by MMP12 at ^{376}L↓F^{377}, which removes the reactive bond between R^{426} and S^{427} that mediates inhibition of thrombin by antithrombin (Björk et al., 1982). Notably, ^{376}L-F^{377} is in the hI/s5A loop and serpin inhibitory control via cleavage at this point, revealing an unexpected mechanism for serpin inhibition. Thus, resident macrophages may promote blood coagulation early following tissue injury through release of MMP12.

The biological and regulatory role for MMP12 in inflammation pathways was revealed from the knockout mice, where perturbations in inflammatory pathways were grossly observed on a macroscopic scale, including accumulation of two new MMP12 substrates, actin and fibrin, and was accompanied by intense neutrophilia. The large infiltrates of neutrophils in the inflamed joints of *Mmp12*$^{-/-}$ mice in collagen-induced arthritis led to a pronounced accumulation of NETs in the extracellular, intra-articular, and marrow spaces that were abnormal: NETs in *Mmp12*$^{-/-}$ mice contained large amounts of fibrin and extracellular actin, which are not normally associated with NETs (Brinkmann et al., 2004). Extracellular actin is a hallmark of inflammatory cell damage, since it is released upon cell death and triggers further inflammatory reactions (Erukhimov et al., 2000). Filamentous actin is removed by a sophisticated actin-scavenging system involving the abundant plasma gelsolin and clearance in the liver (Lee and Galbraith, 1992). However, the critical role of the macrophage and MMP12 in extracellular actin removal has not been previously reported. We found that MMP12 cleaved both actin and gelsolin along with other intracellular proteins (Table 1), adding to the growing list of cytosolic proteins that are cleaved by MMPs in the extracellular space (Butler and Overall, 2009b; 2009a; Cauwe and Opdenakker, 2010). Gelsolin was cleaved into different functional domains that no longer nucleated actin polymerization yet retained actin-severing activity (Figures S7C–S7F), thus revealing concerted roles for MMP12 in countering extracellular actin polymerization and in promoting the clearance of filamentous actin in vivo.

Fibrin deposits in the arthritic joints, a hallmark of early rheumatoid arthritis (Raghu and Flick, 2011), were also more pronounced in the MMP12-knockout mice. We found that MMP12 and PMA-stimulated macrophages rapidly cleared fibrin clots in vitro and that wild-type macrophages were more effective in fibrin dissolution ex vivo than those from knockout mice. Together with the large fibrin deposits in the *Mmp12*$^{-/-}$ mice, this reflects the biological relevance of MMP12 in fibrinolysis in vivo compared to neutrophil fibrinolytic proteases (e.g., elastase and cathepsin G secreted from the dense neutrophil infiltrate in *Mmp12*$^{-/-}$ mice). Thrombin-generated fibrin peptides are chemotactic for monocytes (Richardson et al., 1976), and MMP12 is activated by thrombin and plasmin (Raza et al., 2000), thus forming a proteolytic pathway for fibrin clearance in vivo.

The complement system consists of more than 35 intact or split proteins that recognize and promote elimination of foreign or damaged material, either by opsonization and phagocytosis, or by lysis. Serine complement proteases are long known to cleave and activate complement proteins at canonical sites, seven of which were identified in vivo by TAILS. In addition, we identified undescribed cleavage sites within C3 and other complement proteins, four of which had neo-N-terminal peptides with *Mmp12* WT/KO isotopic ratios indicative of MMP12 processing. C3 is central to all the classical, alternative, and mannose-binding lectin cascades. We validated the TAILS data showing that MMP12 cleaved full-length C3, C3a, C3b, and iC3b in in vitro assays. Although MMP12 also cleaved C4b and factors H and I, MMP12 is not a nonspecific protease, as factor D was not cleaved. Thus, MMP12 cleavage of so many complement proteins indicates the importance of this protease in downregulating complement. We hypothesized that cleavage

A Cleavage sites within gelsolin and actin identified by TAILS

Protein	IPI	P1' residue of cleavage sites in vitro	in vivo
Gelsolin	IPI00117167	50, 51, 58, 327, 357, 404, 408, 431	51, 175, 408, 409
Actin cytoplasmic	IPI00110850	7, 8, 9, 16, 17, 103, 165, 267, 274, 298, 349, 355, 360	356, 357
Actin skeletal	IPI00110827	43, 45, 47, 51, 55, 84, 107, 108, 186, 187, 188, 231 235, 236, 238, 248, 302, 303, 315, 319, 325, 327	

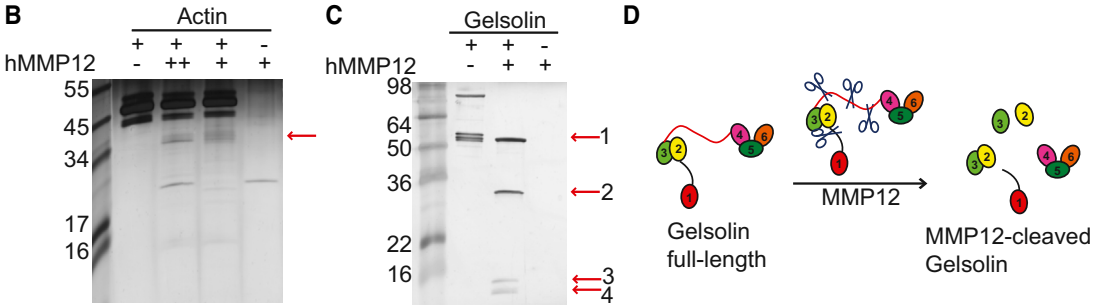

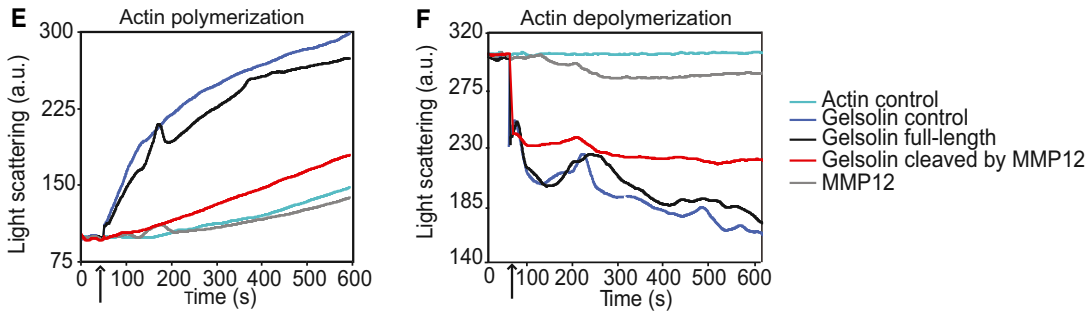

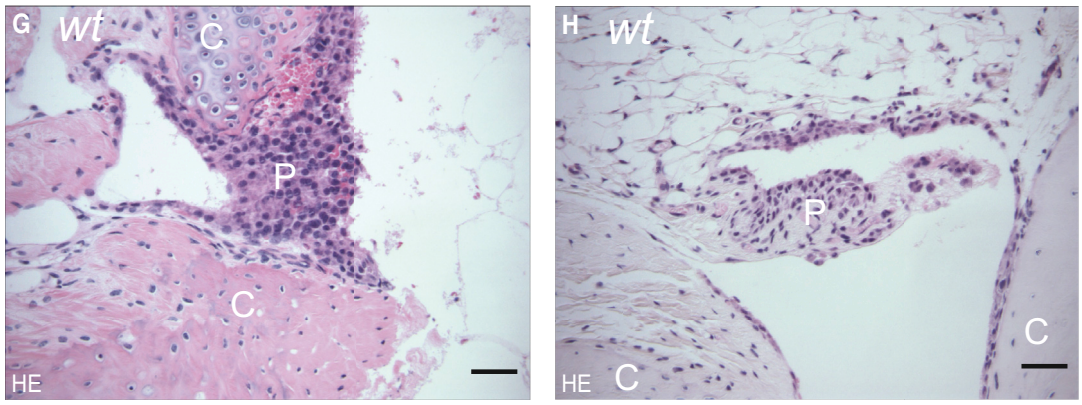

(legend on next page)

A

Cleavage sites within components of the coagulation system identified by TAILS and Edman sequencing

Protein	IPI	P1' residue of cleavage site (TAILS)	Edman
Antithrombin	IPI00136642	33, 34, 35, 36, 37, 377	33
Fibrinogen alpha	IPI00115522	20, 21, 22, 23, 240, 361, 407, 409	
Fibrinogen beta	IPI00279079	20, 307, 392	
Fibrinogen gamma	IPI00122312	67, 380	
Prothrombin	IPI00114206		44

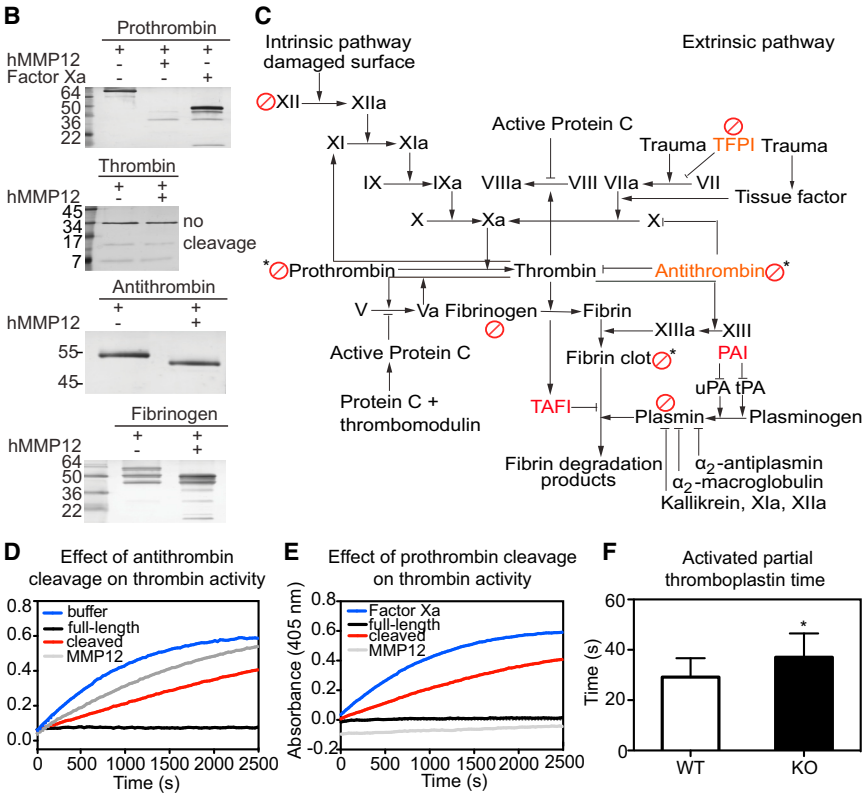

Figure 5. MMP12 Substrates in Blood Coagulation and Fibrinolysis Cascades

(A) Cleavage sites identified by TAILS of murine peritonitis samples. Known mature N termini are in red. Edman, the N terminus of major cleavage products in the in vitro cleavage assays were microsequenced.

(B) Biochemical validation as MMP12 substrates of human prothrombin, bovine antithrombin, and human fibrinogen. Active thrombin is not further cleaved by MMP12.

(C) Schematic of the coagulation and fibrinolysis cascades consisting of the intrinsic and extrinsic pathways that merge at the formation of thrombin activation leading to the formation of fibrin clots. Activated plasmin dissolves fibrin. Red slash circles are MMP12 substrates among which substrates (*) were identified here by TAILS and biochemically validated.

(D) Progress curves of 50 nM active thrombin activity using chromogenic substrate S-2238 in the presence of 500 nM antithrombin (full length) or 500 nM cleaved antithrombin (cleaved).

(E) Thrombin progress curves showing prothrombin activation by MMP12 compared with factor Xa.

(F) Activated partial thromboplastin time was significantly increased in plasma of healthy *Mmp12*$^{-/-}$ mice (n = 4, in duplicate). Values are mean ± SD. *p < 0.05; Mann-Whitney t test.

of iC3b and C3b would reduce phagocytosis of opsonized particles—in fact, the opposite occurred. Cleavage of both iC3b and C3b by MMP12 increased the uptake of serum-opsonized beads by THP1 monocytes. Thus, by enhancing the removal of C3b or iC3b-opsonized pathogens or apoptotic neutrophils in vivo, these inflammation resolution roles of MMP12 are concordant with the effect of MMP12 in dampening complement C3 activity.

C3a and C5a, which are potent chemotactic agents for eosinophils (C3a), mast cells (C3a and C5a), neutrophils (C5a), and macrophages (C5a), were processed by MMP12. The C-terminal

Figure 4. MMP12 Cleavages of Gelsolin and Actin Prevent Actin Polymerization In Vitro and In Vivo

(A) Gelsolin and actin cleavage sites identified by TAILS in MMP12-cleaved secretomes (in vitro) and peritonitis exudate (in vivo).

(B and C) MMP12 cleaves actin (B) and gelsolin (C). Digestion products (red arrows) were separated by 15% Tris-Tricine gels (actin) or 12% SDS-PAGE (gelsolin) and silver stained.

(D) Schematic of the six homologous gelsolin domains (G1–G6) processed by MMP12 into the fragments: G1 plus linker, G2-G3, G2, G3, and G4-G6.

(E) MMP12-cleaved gelsolin loses actin polymerization nucleation activity. Both gelsolin and full-length gelsolin in MMP12 assay buffer efficiently nucleate actin filament growth. G-actin was incubated for 10 min in gel filtration buffer alone (actin control) or after adding the following proteins (protein:actin 100:1 mol ratio) at the time indicated by the arrow: gelsolin in MMP12 buffer alone (full-length gelsolin) or gelsolin in gel filtration buffer alone (gelsolin control); gelsolin cleaved by MMP12 in assay buffer; MMP12 alone with G-actin in assay buffer.

(F) Actin depolymerization assay. The following proteins were added to F-actin at a mol ratio of 1:20 in polymerization buffer at the time indicated by the arrow: buffer alone; gelsolin as a control in gel filtration buffer; full-length gelsolin in MMP12 assay buffer; MMP12-cleaved gelsolin in assay buffer; and MMP12 alone in assay buffer. The sharp drop of light scattering showed that like the gelsolin control and full-length gelsolin, MMP12-cleaved gelsolin retained F-actin severing activity. Day 18 *Mmp12*$^{-/-}$ animals show unresolved tissue clots that contain extracellular actin, DNA, fibrin, and neutrophils.

(G–I) wild-type (WT) (G and H) and *Mmp12*$^{-/-}$ (I) ankle joints with H&E staining showed rich accumulations of dark blue intracellular material that was now extracellular only in *Mmp12*$^{-/-}$ arthritic joints as DNA NETs and that contained prominent neutrophils (white arrows) (see also Figures S6–S8). N, NETs; P, pannus; C, cartilage.

(J and K) Hoechst staining showed extracellular DNA (blue) (J). Alexa 488-phalloidin staining revealed extracellular actin in the NETs (green). Higher-power view of box in (J) showing extensive extracellular actin in arthritis in the knockout mouse (K). Intact cells, including prominent polymorphonuclear leukocytes (pmnl), contained actin in their cytoskeleton.

Original magnification ×400 (G and H) or ×630 (I and J); scale bars represent 25 μm (G and H) and 10 μm (I–K).

octapeptide of C3a triggers activation of the C3a-receptor, and even removal of just the C-terminal arginine abolishes the biological activity of C3a (Hoeprich and Hugli, 1986). We found that MMP12 cleaved C3a to remove eight amino acids from the C terminus, which decreased calcium mobilization 3-fold in THP1 monocytes. C5a was also inactivated by C-terminal processing to reduce calcium mobilization.

Since MMP12 inactivates C3a and C5a and promotes phagocytosis of C3b-and iC3b-opsonized particles upon cleavage, we hypothesized that MMP12 downregulates inflammatory cell infiltration to resolve inflammation and prevent ongoing tissue damage. Indeed, *Mmp12*$^{-/-}$ mice showed significantly greater ankle swelling than wild-type mice in collagen-induced arthritis at 18 days. Histopathological assessment confirmed massive inflammatory cell infiltration. Strikingly, the joints of *Mmp12*$^{-/-}$ mice contained proportionately far more neutrophils than wild-types, whereas macrophage numbers were significantly reduced in *Mmp12*$^{-/-}$ mice (Figure S5) as has been observed previously in different models but attributed to reduced ECM degradation (Goncalves DaSilva and Yong, 2009; Shipley et al., 1996). Notably, overt inflammation in wild-type mice at day 18 was rare, but when present in one mouse, the infiltrate was dominated by macrophages.

Our study shows that in the absence of MMP12, where chemoattractants including C5a are not cleaved and therefore remain active, neutrophils are persistently recruited. Also, neutrophils may not be cleared as readily by phagocytosis due to reduced macrophage numbers and reduced cell surface "eat-me" signals on apoptotic cells. We also demonstrated truncation of immunoglobulin IgG2B by MMP12, which prevents complement activation due to impaired binding of the cleaved form to the Fc receptor, an additional protective effect that is lacking in *Mmp12*$^{-/-}$ mice. Thus, we suggest that neutrophil infiltration into the joint space and effusion of active neutrophil proteases, together with the lack of complement inactivation, is responsible for the advanced destruction of cartilage and subchondral bone in the *Mmp12*$^{-/-}$ mice.

Our TAILS proteomics analyses revealed functions for MMP12 as a procoagulant and in dampening the inflammatory response to favor resolution: MMP12 represses neutrophil infiltration in tissue, reduces complement activation, prevents extracellular actin polymerization, and removes actin filaments and fibrin from NETs to promote homeostasis in vivo. The importance and beneficial role of MMP12 is highlighted in its absence, where unresolved inflammation persists and is exacerbated in vivo in arthritis. The net effect of MMP12 cleavage on several coagulation proteins is to reduce the activated partial thromboplastin time by thrombin activation and in opening a metalloserpin switch by inactivation of antithrombin. Hence, these procoagulant activities of MMP12 exceed the anticoagulant effect of fibrinogen cleavage. Overall, MMP12 is identified as a key mediator that sets the stage for resolution of inflammation, a role very different from its traditionally ascribed role in ECM degradation.

EXPERIMENTAL PROCEDURES

Secretome and Peritoneal Lavage Preparations

Secretomes (500 μg) prepared from 129SvEv *Mmp12*$^{-/-}$ MEFs and RAW 264.7 macrophages were incubated with active murine MMP12 (5 μg) in 50 mM HEPES, 100 mM NaCl, and 5 mM $CaCl_2$ (pH 7.6) at 37°C for 16 hr. The same volume of buffer containing 1 mM APMA was added to control secretomes. Male 42-day *Mmp12*$^{-/-}$ and *Mmp12*$^{+/+}$ mice on the 129SvEv or the B10.RIII background (n = 6 for each of the four genotypes) were injected intraperitoneally with 0.5 ml of sterile 4% thioglycollate. Mice were euthanized 96 hr later, and the peritoneal cavity was washed out with 4 ml sterile PBS. After centrifugation (400 × *g*), the supernatant was treated with 0.5 mM phenylmethanesulfonylfluoride and 1 mM EDTA and TCA precipitated as described in Supplemental Experimental Procedures.

Terminal Amine Isotopic Labeling of Substrates and Mass Spectrometry

MMP12-digested secretome and peritoneal lavage protein samples were denatured, reduced, alkylated, and separately labeled with isotopic iTRAQ-label or CLIP-TRAQ-labels as described in Supplemental Experimental Procedures. The different isotopic-labeled samples were then combined and trypsinized at 37°C for 16 hr. Unblocked unlabeled tryptic peptides were removed by 5-fold excess of a high-molecular-weight polyaldehyde polymer (Kleifeld et al., 2010) (http://flintbox.com/public/project/1948/) and the polymer then removed by ultrafiltration. The unbound N-terminal peptide solution was fractionated by strong-cation exchange high-performance liquid chromatography and analyzed by liquid chromatography-MS/MS on a QSTAR XL Hybrid ESI mass spectrometer (Prudova et al., 2010).

MS2 scans were searched against a mouse International Protein Index (IPI) protein database by Mascot and X!Tandem as described in Supplemental Experimental Procedures. Search results were evaluated by the Trans Proteomic Pipeline using PeptideProphet for peptide/protein identification and Libra for quantification of iTRAQ reporter ion intensities. Final data sets included only peptides with a PeptideProphet probability error rate $\leq$5%.

Proteomic Identification of Cleavage Site Specificity, or PICS

Proteome-derived peptide libraries were prepared for in vitro digestion with MMP12, and the cleaved peptides were N-terminal biotin conjugated for purification and MS/MS analysis as described previously (Schilling and Overall, 2008). MMP12 cleavage site specificities in vivo and in vivo were displayed as heatmaps.

Alternative Pathway Complement Activation by MMP12-Cleaved C3

C3 was incubated with 50 nM MMP12 in HEPES-buffered saline, 4 mM $CaCl_2$ at 37°C for 16 hr. Cleavage reactions were added to C3-deficient human serum, and alternative pathway of complement activation was determined by incubation for 45 min at 37°C with 2.5 × 10^7 rabbit red blood cells (RBCs) in GVB-M_7C_1, 2 mM EDTA and hemolysis quantified from the absorbance at 405 nm as described in Supplemental Experimental Procedures. The hemolytic activity of C3-deficient serum could be fully restored by adding 20–40 nM intact C3.

Proteolytic Cleavage of C3b on RBCs by MMP12 and Alternative Pathway Activation

C3b-tagged RBC (2 × 10^8 cells) in HBS-C_4 were incubated with 0, 1.2, 6.1, 24.2, or 121 nM MMP12; 400 nM factor I or 0, 10, 50, or 400 nM factor I with 2 μM factor H were controls. After 16 hr incubation at 37°C, any MMP12 and cleavage products that were not cell associated were removed by extensive washes. Nontreated and treated C3b-tagged RBCs (2.75 × 10^7 RBCs) were analyzed by hemolysis in C3-deficient serum dependent to determine activation of the alternative pathway and its inhibition by MMP12 as described above and in Supplemental Experimental Procedures.

Phagocytosis Assay

To test the effect of C3b and iC3b cleavage by MMP12 on phagocytosis, human recombinant C3b and iC3b were incubated with human MMP12 at a molar ratio 10:1 at 37°C for 2 hr in the presence or absence of 1 μM marimastat. Samples were then added to human serum-coated Fluoresbrite 2 μm microparticles and incubated with PMA-activated THP1 cells for 1 hr at a final concentration of 5 μM intact or cleaved C3b or iC3b. Phagocytosis was analyzed by flow cytometry as described in Supplemental Experimental Procedures.

Effect of MMP12 Cleavage on Calcium Mobilization by C3a

Intracellular calcium mobilization in response to addition of full-length C3a or MMP12-cleaved C3a to Fluo-4-loaded THP1 cells was measured by fluorometry (excitation 494 nm, emission 514 nm) for 150 s at 37°C followed by addition of 5 μM ionomycin for 150 s to obtain fluorescence manimum (F_{max}) and 20 mM EGTA to obtain fluorescence minimum (F_{min}) as described in Supplemental Experimental Procedures.

The Role of MMP12 in Collagen-Induced Arthritis

Arthritis was induced by collagen injection in CFA in 49-day old male *Mmp12*$^{-/-}$ (n = 15) and *Mmp12*$^{+/+}$ mice (n = 14) on the B10.RIII background. Day 0 is defined as 21 days after collagen injection and was typically the date of onset of arthritis. On day 18, mice were euthanized and hind ankles were dissected and prepared for histological staining by H&E, toluidine blue to visualize cartilage matrix and immunostained as described in Supplemental Experimental Procedures. Standard images were used to score ankle joint inflammation as adapted from the Krenn scheme (Krenn et al., 2006): no inflammation with no synovial increase in cellularity (0); moderate increase in synovial cellularity (1); overt synovial inflammatory infiltrate (2); overt synovial inflammatory infiltrate plus any inflammatory cells in the synovial fluid (3); and abundant infiltration of inflammatory cells into synovial space (4).

Actin Polymerization and Depolymerization Assays

G-actin (4 μM) was preincubated for 10 min alone or at a 100:1 molar ratio with intact or MMP12-cleaved gelsolin in 1.35 ml buffer A (2 mM Tris-HCl, 0.2 mM ATP, 0.2 mM $CaCl_2$, 0.5 mM DTT [pH 7.6]). Light scattering was monitored at 90° to the incident beam using a Perkin Elmer LS55 Luminescence Spectrometer, following addition of 150 μl 10× polymerization buffer (1 M KCl, 20 mM $MgCl_2$), at 360 nm excitation and 364 nm emission with 3.5 nM band passes. Cleavage of gelsolin by MMP12 was performed in 50 mM Tris-HCl, 150 mM NaCl, and 5mM $CaCl_2$ (pH 7.6) at 37°C for 16 hr, which was then added to buffer A. Assays were performed in triplicate and the experiment repeated twice.

For actin depolymerization, G-actin (4 μM) was polymerized by incubation for 1 hr after addition of polymerization buffer to 1×. Test proteins then were added at a 1:20 mol ratio of protein:actin in a final volume of 1.5 ml. Light scattering was measured as above.

Thrombin Assay

Thrombin activity was quantified at A_{405} nm after the addition of 100 μM chromogenic substrate (H-D-Phe-Pip-Arg-pNA, Chromogenix) to 50 nM human thrombin that had been preincubated for 10 min with 2 nM heparin (Iduron) in 20 mM PBS (pH 7.4), 100 mM NaCl, 0.1% Tween 20, and 0.1% BSA at 22°C. Prothrombin activation was assessed by incubating 400 nM prothrombin with 40 nM human MMP12 or 4 nM factor Xa in assay buffer containing 5 mM $CaCl_2$ at 37°C for 16 hr before the addition of 100 μM thrombin substrate. To test the effect of antithrombin cleavage by MMP12, 500 nM bovine antithrombin was incubated with 50 nM human MMP12 (or buffer) in 20 mM HEPES, 100 mM NaCl, and 5 mM $CaCl_2$ for 16 hr at 37°C, before the addition of thrombin. After incubation for 30 min, thrombin activity was quantified as above.

Fibrin Clot Formation

A total of 1 nM human thrombin was added to 2.9 μM human fibrinogen in 20 mM HEPES, 100 mM NaCl, 5 mM $CaCl_2$, and 0.01% Tween 20 (pH 7.4) on ice, and fibrin clot formation was quantified by the increase in A_{405} nm. To test the effect of MMP12 on clotting, fibrinogen was preincubated with MMP12 (or buffer) at a 10:1 mol ratio at 37°C, 16 hr before adding thrombin.

Fibrinolysis

After 1 hr fibrin clot formation, hMMP12 (mol ratio 10:1), MMP12 preincubated with marimastat (1 μM), or buffer was added in a volume of 5 μl to the fibrin clot, and the decrease in A_{405} nm was measured. Peritoneal macrophages were isolated from *Mmp12*$^{-/-}$ (n = 5) and *Mmp12*$^{+/+}$ (n = 5) mice 96 hr after thioglycollate stimulation as described in Supplemental Experimental Procedures. Two hours after fibrin clot formation, 1 × 10^4 wild-type or knockout macrophages were added to each well containing fibrin clots (n = 11/condition) and incubated for 2 hr or 4 hr. Cells were then removed, and remaining fibrin clots were fixed by 4% formaldehyde.

Activated Partial Thromboplastin Time

Male *Mmp12*$^{-/-}$ and *Mmp12*$^{+/+}$ (B10.RIII background, n = 4 each) mouse plasma (50 μl) was diluted with 50 μl Hank's balanced salt solution before the addition of 50 μl prewarmed partial thromboplastin time reagent (STAGO) followed by incubation at 37°C for 3 min. Clotting was induced by addition of 50 μl prewarmed 25mM $CaCl_2$, and clotting time measured in a STAGO ST4 analyzer. Samples were measured in duplicate.

SUPPLEMENTAL INFORMATION

Supplemental Information includes Supplemental Results, Supplemental Experimental Procedures, seven figures, and one table and can be found with this article online at http://dx.doi.org/10.1016/j.celrep.2014.09.006.

AUTHOR CONTRIBUTIONS

C.L.B. performed and analyzed most of the experiments and wrote the manuscript. A.D. performed cleavage assays, phagocytosis, calcium flux, isolation of peritoneal macrophages, fibrinolysis assays, and immunohistochemistry. M.J.K. performed the complement hemolysis assays. C.R.R. performed histological assessments and immunohistochemistry and helped with data interpretation. A.L. expressed and purified human gelsolin and performed actin polymerization and depolymerization assays. G.S.B. helped with the isolation of peritoneal macrophages and edited the manuscript. A.E.S. participated in the arthritis experiments. P.T.L. performed GO analysis and helped with data interpretation. U.a.d.K. developed the statistical software for MS-data analysis. V.G. performed some biochemical cleavage assays. R.G.K. managed the mouse colony and performed genotyping. L.D.B. and E.M.C. provided scientific input for the project. C.M.O. designed the project and was responsible for project supervision and data interpretation and wrote the manuscript.

ACKNOWLEDGMENTS

We thank Drs. W Chen and J. Rogalski for mass spectrometer operation, J. Kizhakkedathu for the HPG-ALD polymer, and D. Marchant (University of Alberta) for insightful discussions. C.M.O. holds a Canada Research Chair in Metalloproteinase Proteomics and Systems Biology. E.M.C. holds a CSL-Behring Research Chair and a Canada Research Chair in Endothelial Cell Biology. This work was supported by a grant from the CIHR and NSERC as well as an Infrastructure Grant from MSHFR and the Canada Foundations for Innovation.

Received: June 9, 2014
Revised: July 2, 2014
Accepted: September 2, 2014
Published: October 9, 2014

REFERENCES

auf dem Keller, U., and Overall, C.M. (2012). CLIPPER: an add-on to the TopFIND Proteomic Pipeline for the automated analysis of TAILS N-terminomics data. Biol. Chem. *393*, 1477–1483.

auf dem Keller, U., Prudova, A., Gioia, M., Butler, G.S., and Overall, C.M. (2010). A statistics-based platform for quantitative N-terminome analysis and identification of protease cleavage products. Mol. Cell. Proteomics *9*, 912–927.

auf dem Keller, U., Prudova, A., Eckhard, U., Fingleton, B., and Overall, C.M. (2013). Systems-level analysis of proteolytic events in increased vascular permeability and complement activation in skin inflammation. Sci. Signal. *6*, rs2.

Björk, I., Jackson, C.M., Jörnvall, H., Lavine, K.K., Nordling, K., and Salsgiver, W.J. (1982). The active site of antithrombin. Release of the same proteolytically

cleaved form of the inhibitor from complexes with factor IXa, factor Xa, and thrombin. J. Biol. Chem. *257*, 2406–2411.

Brinkmann, V., Reichard, U., Goosmann, C., Fauler, B., Uhlemann, Y., Weiss, D.S., Weinrauch, Y., and Zychlinsky, A. (2004). Neutrophil extracellular traps kill bacteria. Science *303*, 1532–1535.

Butler, G.S., and Overall, C.M. (2009a). Updated biological roles for matrix metalloproteinases and new "intracellular" substrates revealed by degradomics. Biochemistry *48*, 10830–10845.

Butler, G.S., and Overall, C.M. (2009b). Proteomic identification of multitasking proteins in unexpected locations complicates drug targeting. Nat. Rev. Drug Discov. *8*, 935–948.

Cauwe, B., and Opdenakker, G. (2010). Intracellular substrate cleavage: a novel dimension in the biochemistry, biology and pathology of matrix metalloproteinases. Crit. Rev. Biochem. Mol. Biol. *45*, 351–423.

Dean, R.A., Cox, J.H., Bellac, C.L., Doucet, A., Starr, A.E., and Overall, C.M. (2008). Macrophage-specific metalloelastase (MMP-12) truncates and inactivates ELR+ CXC chemokines and generates CCL2, -7, -8, and -13 antagonists: potential role of the macrophage in terminating polymorphonuclear leukocyte influx. Blood *112*, 3455–3464.

Erukhimov, J.A., Tang, Z.L., Johnson, B.A., Donahoe, M.P., Razzack, J.A., Gibson, K.F., Lee, W.M., Wasserloos, K.J., Watkins, S.A., and Pitt, B.R. (2000). Actin-containing sera from patients with adult respiratory distress syndrome are toxic to sheep pulmonary endothelial cells. Am. J. Respir. Crit. Care Med. *162*, 288–294.

Fortelny, N., Cox, J.H., Kappelhoff, R., Starr, A.E., Lange, P.F., Pavlidis, P., and Overall, C.M. (2014). Network analyses reveal pervasive functional regulation between proteases in the human protease web. PLoS Biol. *12*, e1001869.

Galli, S.J., Borregaard, N., and Wynn, T.A. (2011). Phenotypic and functional plasticity of cells of innate immunity: macrophages, mast cells and neutrophils. Nat. Immunol. *12*, 1035–1044.

Geissmann, F., Manz, M.G., Jung, S., Sieweke, M.H., Merad, M., and Ley, K. (2010). Development of monocytes, macrophages, and dendritic cells. Science *327*, 656–661.

Goncalves DaSilva, A., and Yong, V.W. (2009). Matrix metalloproteinase-12 deficiency worsens relapsing-remitting experimental autoimmune encephalomyelitis in association with cytokine and chemokine dysregulation. Am. J. Pathol. *174*, 898–909.

Gronski, T.J., Jr., Martin, R.L., Kobayashi, D.K., Walsh, B.C., Holman, M.C., Huber, M., Van Wart, H.E., and Shapiro, S.D. (1997). Hydrolysis of a broad spectrum of extracellular matrix proteins by human macrophage elastase. J. Biol. Chem. *272*, 12189–12194.

Gulla, K.C., Gupta, K., Krarup, A., Gal, P., Schwaeble, W.J., Sim, R.B., O'Connor, C.D., and Hajela, K. (2010). Activation of mannan-binding lectin-associated serine proteases leads to generation of a fibrin clot. Immunology *129*, 482–495.

Hiller, O., Lichte, A., Oberpichler, A., Kocourek, A., and Tschesche, H. (2000). Matrix metalloproteinases collagenase-2, macrophage elastase, collagenase-3, and membrane type 1-matrix metalloproteinase impair clotting by degradation of fibrinogen and factor XII. J. Biol. Chem. *275*, 33008–33013.

Hoeprich, P.D., Jr., and Hugli, T.E. (1986). Helical conformation at the carboxy-terminal portion of human C3a is required for full activity. Biochemistry *25*, 1945–1950.

Houghton, A.M.A., Hartzell, W.O.W., Robbins, C.S.C., Gomis-Rüth, F.X.F., and Shapiro, S.D.S. (2009). Macrophage elastase kills bacteria within murine macrophages. Nature *460*, 637–641.

Kleifeld, O., Doucet, A., auf dem Keller, U., Prudova, A., Schilling, O., Kainthan, R.K., Starr, A.E., Foster, L.J., Kizhakkedathu, J.N., and Overall, C.M. (2010). Isotopic labeling of terminal amines in complex samples identifies protein N-termini and protease cleavage products. Nat. Biotechnol. *28*, 281–288.

Krenn, V., Morawietz, L., Burmester, G.-R., Kinne, R.W., Mueller-Ladner, U., Muller, B., and Haupl, T. (2006). Synovitis score: discrimination between chronic low-grade and high-grade synovitis. Histopathology *49*, 358–364.

Lee, W.M., and Galbraith, R.M. (1992). The extracellular actin-scavenger system and actin toxicity. N. Engl. J. Med. *326*, 1335–1341.

Liu, Y., Zhang, M., Hao, W., Mihaljevic, I., Liu, X., Xie, K., Walter, S., and Fassbender, K. (2013). Matrix metalloproteinase-12 contributes to neuroinflammation in the aged brain. Neurobiol. Aging *34*, 1231–1239.

Marchant, D.J., Bellac, C.L., Moraes, T.J., Wadsworth, S.J., Dufour, A., Butler, G.S., Bilawchuk, L.M., Hendry, R.G., Robertson, A.G., Cheung, C.T., et al. (2014). A new transcriptional role for matrix metalloproteinase-12 in antiviral immunity. Nat. Med. *20*, 493–502.

Prudova, A., auf dem Keller, U., Butler, G.S., and Overall, C.M. (2010). Multiplex N-terminome analysis of MMP-2 and MMP-9 substrate degradomes by iTRAQ-TAILS quantitative proteomics. Mol. Cell. Proteomics *9*, 894–911.

Raghu, H., and Flick, M.J. (2011). Targeting the coagulation factor fibrinogen for arthritis therapy. Curr. Pharm. Biotechnol. *12*, 1497–1506.

Raza, S.L., Nehring, L.C., Shapiro, S.D., and Cornelius, L.A. (2000). Proteinase-activated receptor-1 regulation of macrophage elastase (MMP-12) secretion by serine proteinases. J. Biol. Chem. *275*, 41243–41250.

Richardson, D.L., Pepper, D.S., and Kay, A.B. (1976). Chemotaxis for human monocytes by fibrinogen-derived peptides. Br. J. Haematol. *32*, 507–513.

Schilling, O., and Overall, C.M. (2008). Proteome-derived, database-searchable peptide libraries for identifying protease cleavage sites. Nat. Biotechnol. *26*, 685–694.

Shipley, J.M., Wesselschmidt, R.L., Kobayashi, D.K., Ley, T.J., and Shapiro, S.D. (1996). Metalloelastase is required for macrophage-mediated proteolysis and matrix invasion in mice. Proc. Natl. Acad. Sci. USA *93*, 3942–3946.

Soehnlein, O., and Lindbom, L. (2010). Phagocyte partnership during the onset and resolution of inflammation. Nat. Rev. Immunol. *10*, 427–439.

Wang, Q., Rozelle, A.L., Lepus, C.M., Scanzello, C.R., Song, J.J., Larsen, D.M., Crish, J.F., Bebek, G., Ritter, S.Y., Lindstrom, T.M., et al. (2011). Identification of a central role for complement in osteoarthritis. Nat. Med. *17*, 1674–1679.